

Age-hardening and overaging mechanisms related to the metastable phase formation by the decomposition of Ag and Cu in a dental Au–Ag–Cu–Pd–Zn alloy

Sang-Hwa Lee · In-Sook Lim · Mi-Hyang Cho ·
Ae-Ri Pyo · Yong Hoon Kwon · Hyo-Joung Seol ·
Hyung-Il Kim

Published online: 7 July 2011

© The Author(s) 2011. This article is published with open access at Springerlink.com

Abstract The age-hardening and overaging mechanisms related to the metastable phase formation by the decomposition of Ag and Cu in a dental casting gold alloy composed of 56Au–25Ag–11.8Cu–5Pd–1.7Zn–0.4Pt–0.1Ir (wt.%) were elucidated by characterizing the age-hardening behaviour, phase transformations, changes in microstructure and changes in element distribution. The fast and apparent increase in hardness at the initial stage of the aging process at 400°C was caused by the nucleation and growth of the metastable Ag–Au-rich phase and the Cu–Au-rich phase by the miscibility limit of Ag and Cu. The transformation of the metastable Ag–Au-rich phase into the stable Ag–Au-rich phase progressed concurrently with the ordering of the Cu–Au-rich phase into the AuCu I phase through the metastable state, which resulted in the subsequent increase in hardness. The further increase in hardness was restrained before complete decomposition of the parent α_0 phase due to the initiation of the lamellar-forming grain boundary reaction. The progress of the lamellar-forming grain boundary reaction was not directly connected with the phase transformation of the metastable phases into the final product phases. The heterogeneous expansion of the lamellar structure from the grain boundary caused greater

softening than the subsequent further coarsening of the lamellar structure. The lamellar structure was composed of the Ag–Au-rich layer which was Cu-, Pd- and Zn-depleted and the AuCu I layer containing Pd and Zn.

Keywords Metastable phase · Lamellar-forming grain boundary reaction · Age-hardening mechanism · Overaging · Au–Ag–Cu–Pd–Zn

Introduction

Age-hardenability in age-hardenable dental casting gold alloys is usually obtained in Au–Cu and Ag–Cu systems. In the Au–Cu system, the alloy is hardened by forming the AuCu I ordered structure, where alternate (002) planes are occupied by either all gold or all copper atoms [1]. As the atomic size of Au and Cu is different, such an arrangement in the disordered matrix results in a formation of strain field with lattice distortion. Thus, when the ordered domain grows larger after prolonged aging, the special softening mechanism, that is, twinning occurs to release the lattice distortion [1]. In the Ag–Cu system, the alloy is hardened by the phase separation mechanism due to the miscibility limit of the Ag–Cu system during the aging process [2]. The softening mechanism in the Ag–Cu alloy after prolonged aging is microstructural coarsening to release the lattice distortion in the inter-phase boundaries [2]. However, in most dental casting gold alloys, both Au–Cu and Ag–Cu systems work due to their complex compositions. Thus, the separation into the Ag–Au-rich and Cu–Au-rich phases occurs prior to the ordering into the AuCu I superlattice by the phase separation mechanism such as a spinodal decomposition and a nucleation and growth

S.-H. Lee · I.-S. Lim · A.-R. Pyo · Y. H. Kwon · H.-J. Seol ·
H.-I. Kim (✉)

Department of Dental Materials, School of Dentistry and Medical
Research Institute, Pusan National University,
Beomeo-Ri, Mulgeum-Eup,
Yongsan-Si, Gyeongsangnam-Do 626–814, South Korea
e-mail: seol222@pusan.ac.kr

M.-H. Cho
Department of Dental Lab, Wonkwang Health Science University,
344-2 Sinyong-Dong,
Jeonbuk 570–750, South Korea

mechanism [3–5]. During the phase separation and ordering, the metastable phase could appear depending on the gap in the lattice parameters between the parent phase and the product phases. If the final product phases have a large gap in the lattice parameters with the parent phase, one or more metastable phases will be formed before the final product phases, which will result in a more complicated age-hardening mechanism. Moreover, the increasing Ag content in the Au–Cu system changes the softening mechanism of the alloy from twinning to lamellar formation [6].

In a study on the age-hardening mechanism of a 55Au–19.9Ag–17Cu–4Zn–3Pd (wt.%) alloy aged at 400°C, the spinodal decomposition of the parent phase into the Ag-rich phase and the Cu-rich phase occurred in an instant, and causing a rapid increase in hardness and an apparent delay in softening due to the uniform fine spinodal structure [7]. The formation of the metastable phase was apparent only for the Ag-rich phase in the alloy, which was thought to have resulted from the fact that the gap in the lattice parameter between the parent phase and the final Ag-rich phase was twice larger than that between the parent phase and the final Cu-rich phase. In a study on the age-hardening mechanism of a 68Au–15Cu–6Ag–3Pd–3Zn (wt.%) alloy aged in the temperature range of 200–500°C by Tani et al. [5], the formation of the metastable AuCu I' platelet containing Pt and Pd resulted in an apparent age-hardening by introducing coherency strains in the matrix even though the subsequent softening related to the lamellar formation was not elucidated. In a study on a 30Au–30Ag–20Cu–20Pd (wt.%) alloy aged at 450°C, two metastable phases of Ag-rich' and AuCu I' caused a rapid hardening by introducing coherency strains at the inter-phase boundaries and then an apparent softening by overaging [4]. In a study on a 66Au–18.5Ag–8.5Cu–4.3Pd (wt.%) alloy aged at 400°C, the slow formation of the metastable AuCu I' phase was responsible for the slow and constant hardening [3]. From those studies on the age-hardening mechanism in the Au–Ag–Cu system, it is understandable that the slight variation in the atomic ratio of Cu to Au and to Ag in addition to minor ingredients changes the process of phase transformation and the mechanism of age-hardening and subsequent softening.

In the present study, we investigated a dental casting gold alloy composed of 56Au–25Ag–11.8Cu–5Pd–1.7Zn–0.4Pt–0.1Ir (wt.%). If the separation of Ag and Cu occurs by spinodal decomposition, an apparently rapid hardening and delayed softening will be observed, and if the separation of Ag and Cu occurs by the nucleation and growth mechanism, the age-hardening rate will be variable, mainly depending on the gap between the alloy composition and the composition range having a single phase in the ternary Au–Ag–Cu phase diagram [3, 8]. The purpose of

the present study is to elucidate the age-hardening and overaging mechanisms in the Au–Ag–Cu–Pd–Zn alloy containing Pt and Ir by means of the hardness test, X-ray diffraction (XRD) study, field emission-scanning electron microscopic (FE-SEM) observation and energy dispersive spectrometer (EDS) analysis.

Materials and methods

Specimen alloy

The alloy used in the present study was a dental gold alloy of yellow color (Solaro 3; Metalor Technologies, Switzerland) for crown and bridge fabrication, which belongs to Type 3 alloy by the ISO classification (ISO 22674:2006 (E)). The chemical composition of the alloy is listed in Table 1. The alloy samples were used in the form of small square pieces 8×8×1 mm in a rolled and annealed condition.

Hardness test

Before hardness testing, the alloy samples were solution-treated at 700°C for 10 min under an argon atmosphere, then rapidly quenched into iced brine to prevent any reaction occurring. Then the samples were isochronally aged in the temperature range of 250–500°C, and were isothermally aged at 400°C for various periods of time in a molten salt bath (25% KNO₃+30% KNO₂+25% NaNO₃+20% NaNO₂) which was used for the temperature range 150–550°C, and then quenched into ice brine for subsequent hardness testing. Hardness measurements were made using a Vickers micro-hardness tester (MVK-H1, Akashi Co., Japan) with a load of 300 gf and a dwell time of 10 s. All results were the average values of five measurements.

X-ray diffraction study

For the XRD study, the powder specimens at 300 mesh were produced by filing sample pieces. After being vacuum-sealed in a silica tube and solution-treated at 700°C for 10 min, they were isothermally aged at 400°C for various periods of time in a molten salt bath, and then

Table 1 Chemical composition of the alloy

Solaro 3	Composition						
	Au	Ag	Cu	Pd	Zn	Pt	Ir
wt.%	56.0	25.0	11.8	5.0	1.7	0.4	0.1
at.%	36.6	29.8	23.9	6.0	3.3	0.3	0.1

quenched into ice brine. The XRD profiles were recorded by an X-ray diffractometer (XPERT-PRO; Philips, Netherlands) which was installed at Korea Basic Science Institute, Pusan Center and operated at 30 kV and 40 mA using Nickel-filtered Cu K α radiation. The scanning rate of a goniometer was 2° (2 θ /min).

Field emission scanning electron microscopic observation

For FE-SEM observations, the plate-like samples were subjected to the required heat treatment, and then they were prepared by utilizing a standard metallographic technique. A freshly prepared aqueous solution of 10% potassium cyanide (KCN) and 10% ammonium persulfate ((NH₄)₂S₂O₈) was utilized for the final etching of the samples. The specimens were examined at 20 kV using a field emission scanning electron microscope (JSM-6700F; JEOL, Japan) which was installed at Pukyong National University.

Energy dispersive spectrometer analysis

EDS analysis was carried out to observe the distributional changes of each element in the specimen during the aging process. An energy dispersive X-ray spectrometer (INCA x-sight; Oxford Instruments, UK) of a field emission scanning electron microscope (JSM-6700F; JEOL, Japan) was used at 15 kV to examine the plate-like specimens which were used for the FE-SEM observation.

Results and discussion

Age-hardening behaviour

In order to determine the appropriate aging temperature for the specimen, the plate-like specimens were isochronally aged in the temperature range of 250–500°C. Figure 1 shows the isochronal age-hardening curves of the specimen solution-treated at 700°C for 10 min, and then aged in the temperature range of 250–500°C for 10 min and 20 min. The specimen showed an apparent age-hardenability at 400°C. Therefore, the age-hardening behaviour was observed at 400°C.

In Fig. 2, the isothermal age-hardening curve of the specimen solution-treated at 700°C for 10 min and then aged at 400°C is shown. The hardness increased apparently without latent periods from the initial stage of the aging. By aging the solution-treated specimen at 400°C for 30 s, the hardness increased apparently from 166 to 260 (Hv). By further aging until 20 min, the hardness increased gradually up to the maximum, 283 (Hv), however, the rate of increase slowed. After reaching the maximum hardness value, the

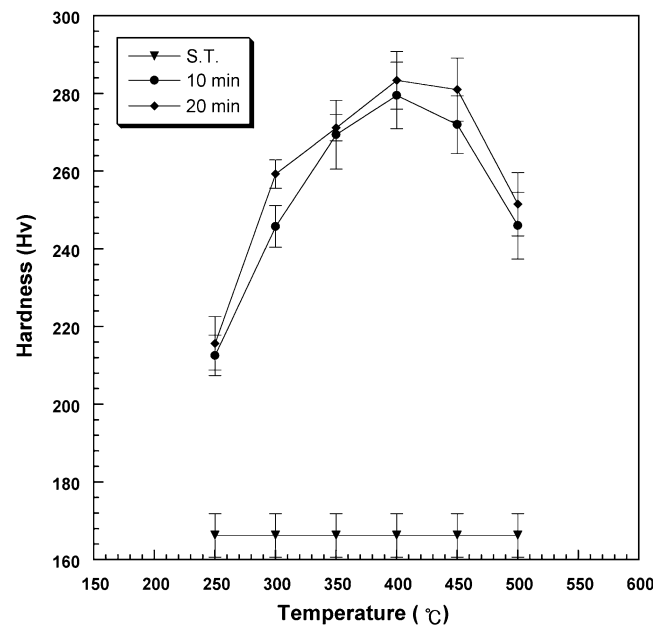


Fig. 1 Isochronal age-hardening curves of subject alloy aged in temperature range of 250–500°C for 10 and 20 min

hardness decreased constantly to 214 (Hv) by further aging until 20,000 min.

Phase transformation

To clarify the mechanism of age-hardening and softening by overaging, the XRD pattern changes during the aging process were examined. Figure 3 shows the variations of the XRD pattern during the isothermal aging at 400°C with

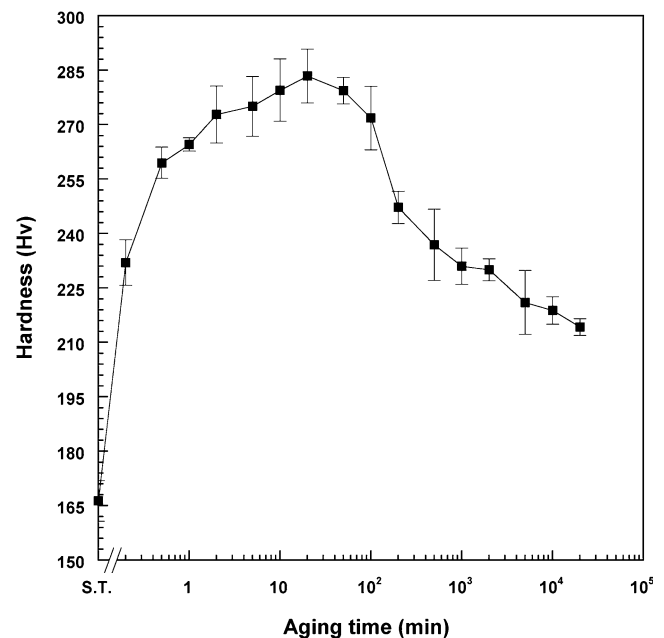


Fig. 2 Isothermal age-hardening curve of subject alloy aged at 400°C

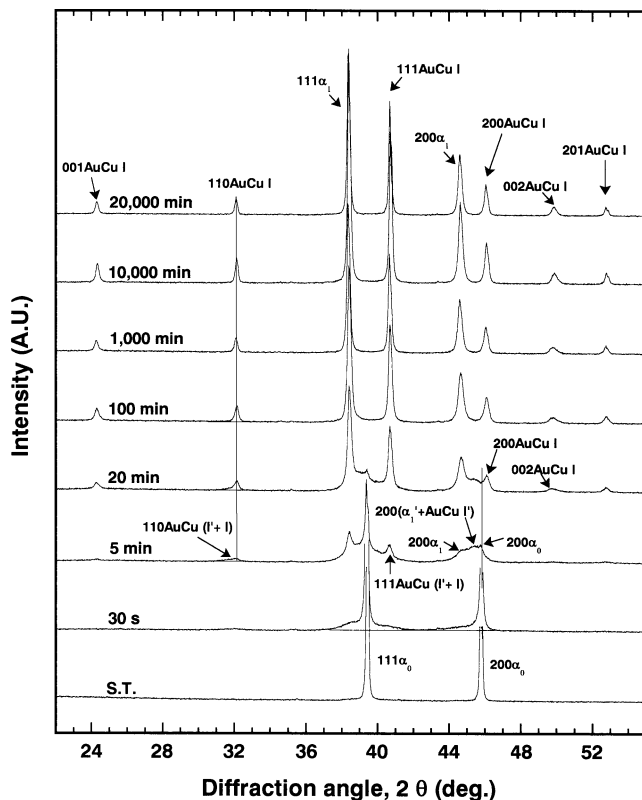


Fig. 3 Variations of the XRD pattern during the isothermal aging at 400°C with aging time

aging time. In the sample solution-treated at 700°C for 10 min, the single face-centered cubic (fcc) α_0 phase with a lattice parameter of $a_{200}=0.3965$ nm was obtained. By aging the specimen at 400°C for 20,000 min, the parent α_0 phase was decomposed into an fcc Ag–Au-rich α_1 phase with $a_{200}=0.4061$ nm and a face-centered tetragonal (fct) AuCu I ordered phase with $a_{200}=0.3940$ nm and axial ratio, $c/a=0.928$.

The variations of the XRD pattern during the isothermal aging at 400°C were examined with respect to the isothermal age-hardening curve at 400°C (Fig. 2). By aging for 30 s when the hardness increased apparently, broad peaks of Ag–Au-rich and Cu–Au-rich were observed at both sides of the parent α_0 phase, and there was no characteristic side-band by spinodal decomposition [7]. In the present study, the alloy is mainly composed of the Au–Ag–Cu system, in which Ag and Cu have a miscibility limit, while Au has complete miscibility with Ag and Cu in the solid state [9]. Thus, it can be thought that a rapid and significant increase in hardness within 30 s was caused by lattice strains formation during the nucleation and growth of the Ag–Au-rich and Cu–Au-rich phases by the miscibility limit of Ag and Cu with the help of quenched-in excess vacancies [6].

At the aging time of 5 min, the (111) peaks of the Ag–Au-rich α_1 and AuCu I phases became apparent even

though the parent (111) α_0 peak was still stronger in its intensity. The newly appeared (110) AuCu I peak ($2\theta\approx 32^\circ$) was broad-shaped toward the lower diffraction angle side. This indicated that the (110) peak of the AuCu I phase was overlapped with that of the metastable AuCu I' phase which has a larger lattice parameter (a) than that of the AuCu I phase. Here, the prime (') symbol refers to a metastable phase. The shape of parent (200) α_0 peak also broadened toward lower diffraction angle side due to the overlap with the (200) metastable α'_1 and stable α_1 peaks. Thus, it is clear that the stable α_1 phase formed from the metastable state. The lattice parameter size of the metastable α'_1 phase was located between that of the parent α_0 and stable α_1 phases, as can be seen from the (200) peak position. Thus, the formation of the metastable phase during the process of phase transformation could possibly attenuate the inter-phase boundary energy by reducing the gap in the lattice parameters. Such an Ag-rich metastable phase formation during the decomposition of Ag and Cu in dental gold alloys has been reported occasionally in the spinodally decomposed alloy and the alloy decomposed by the nucleation and growth mechanism [4, 10]. The AuCu I-type ordered phase has a tetragonality which is the most common mechanism of age-hardening in dental gold alloys [4, 10–13]. However, the degree of ordering of the AuCu I phase at 5 min was too low, as can be seen from the very weak superlattice reflections. Moreover, the metastable AuCu I' phase had common 200 peak with the Ag-rich α'_1 phase. Thus, the lattice distortion in the inter-phase boundaries between the metastable α'_1 phase and the metastable AuCu I' phase must have been minimized.

At the aging time of 20 min when the maximum hardness value was obtained, the peak intensity of the parent α_0 phase became weaker than that of the final product α_1 and AuCu I phases. The ordering of the AuCu I phase progressed sufficiently at the aging time of 20 min, from the strong superlattice reflections. As the parent (200) α_0 peak becomes weak, the (200) and (002) AuCu I peaks appeared clearly in the higher diffraction angle side of the parent (200) α_0 peak. And the (200) peak of the stable α_1 phase became stronger than that of the metastable α'_1 phase. Thus, it can be said that the transformation of the metastable α'_1 phase into the stable α_1 phase progressed concurrently with the ordering of the Cu–Au-rich phase into the AuCu I phase through the metastable state. Such a process must have significantly increased the lattice strains in the inter-phase boundaries between the stable α_1 and AuCu I phases having tetragonality. However, the hardness increasing rate became slow and finally stopped before the complete decomposition of the parent α_0 phase. This indicated that the release of lattice strains was initiated against the accumulated lattice strains in the matrix. At the aging time of 100 min when the hardness decreased slightly

from 283 (Hv) down to 272 (Hv), the (200) diffraction peaks of the parent α_0 and metastable α'_1 phases disappeared, and those of the stable α_1 and AuCu I phases were somewhat broad-shaped yet. By further aging until 20,000 min, the hardness decreased constantly down to 214 (Hv), and all the diffraction peaks grew sharp without any change in position. The sharpening of the broad diffraction peaks indicates the release of the accumulated lattice strains or the changes in the crystallite size [14–16]. In the present case, in the overaging stage from 100 to 20,000 min, no metastable α'_1 nor AuCu I' phases in which large lattice strains were accumulated remained in the alloy. Thus, it can be thought that the continuous decrease in hardness in the later stage of the aging process was related to the continuous microstructural coarsening after the phase transformation. To clarify, the microstructural changes during the aging process were observed.

Microstructural changes

Figure 4 shows the FE-SEM micrographs at a magnification of 5,000 \times (1) and 20,000 \times (2) for the specimens solution-treated at 700°C for 10 min (a) and aged at 400°C for 20 min (b), 100 min (c), 1,000 min (d) and 20,000 min (e). In the solution-treated specimen (Fig. 4a), equiaxed structure of a single phase was observed. At 20 min aging (Fig. 4b) when the hardness had increased to its maximum, the lamellar-forming grain boundary reaction was initiated, and the changes in the grain interior were not clear. The corresponding XRD pattern showed that the parent α_0 phase was not completely transformed into the final product phases, and thus, the specimen was composed of the five phases of the parent α_0 , metastable α'_1 , stable α_1 , metastable AuCu I' and AuCu I even though the most part was composed of the stable α_1 and AuCu I phases. From this, it seemed that the single-phased grain interior was homogeneously decomposed into the metastable Ag–Au-rich α'_1 and Cu–Au-rich phases at a fine scale, and then subsequently transformed into the stable Ag–Au-rich α_1 phase and the AuCu I ordered phase through the metastable state without apparent microstructural changes except for the formation of the lamellar structure in the limited areas of the grain boundaries. The gap in the lattice parameter grew severe with the progress of the phase transformation, and thus, the hardness should have increased until the phase decomposition was completed. However, the further increase in hardness was restrained before the complete decomposition of the parent α_0 phase. This was the result of initiated lamellar-forming grain boundary reaction. The grain boundary lamellar structure has a much coarser nature compared to the grain interior, which means that the phase boundaries between the metastable Ag–Au-rich α'_1 phase and the metastable AuCu I' phase containing lattice strains

were reduced significantly as the grain interior was replaced by the lamellar structure, resulting in the softening [17–19]. The accumulated lattice strains in the matrix seemed to be the driving force for the lamellar-forming grain boundary reaction. From the hardness decrease combined by such a microstructural change, it can be said that the heterogeneous expansion of the lamellar structure from the grain boundary released the lattice strains efficiently by consuming the grain interior.

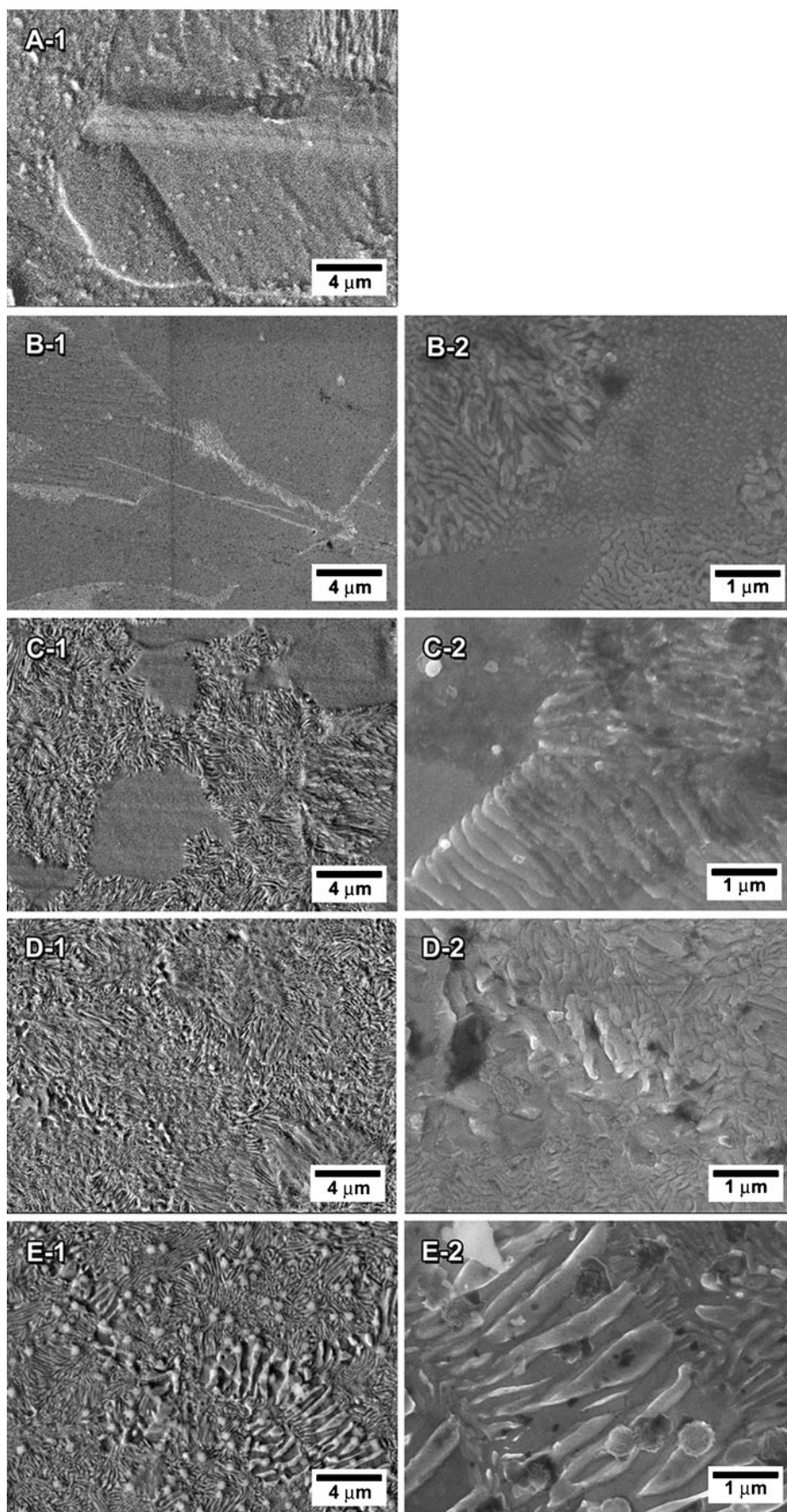
By further aging until 100 min (Fig. 4c) when the hardness decreased slightly from the maximum, 283 down to 272 (Hv), the grain boundaries lamellar structure expanded toward the grain interior. As a result, more than half the matrix was replaced by the lamellar structure. In the corresponding XRD pattern, the phase transformation was completed. Thus, both the grain interior and the lamellar structure were composed of the same final phases of the stable Ag–Au-rich α_1 and AuCu I with high tetragonality. From such a fact, it is clear that the progress of the lamellar-forming grain boundary reaction was not directly connected with the phase transformation of the metastable phases into the final product phases unlike the study with the 30Au–30Ag–20Cu–20Pd (wt.%) alloy [4].

By further aging until 1,000 min (Fig. 4d) when the hardness decreased apparently, the grain interior was completely replaced by the lamellar structure. In the corresponding XRD pattern, there was no further change in the diffraction peak except for the peak sharpening, which indicated that the decrease in hardness was in proportion to the area replaced by the lamellar structure. In the specimen aged for 20,000 min (Fig. 4e) when the hardness was further decreased, the lamellar structure which covered the whole matrix was further coarsened compared to that aged for 1,000 min (Fig. 4d). As the phase transformation had already finished at 100 min, the hardness change after that time was related only to the microstructural changes. By comparing the decreasing rate of hardness until 1,000 and 20,000 min, it can be said that the expansion of the lamellar structure caused greater softening than the subsequent further coarsening of the lamellar structure. Such a subsequent further coarsening after the expansion of the lamellar structure was not observed in the studies on the 30Au–30Ag–20Cu–20Pd (wt.%) alloy aged at 450°C for 20,000 min and the 61Au–20Ag–13Cu–3.3Pd (wt.%) alloy aged at 400°C for 20,000 min, which showed a similar phase transformation process with the present study [4, 10].

Element distribution

EDS analysis of FE-SEM was carried out in order to examine the element distribution in the solute-depleted matrix layer and precipitate layer of the coarse lamellar

Fig. 4 FE-SEM micrographs at a magnification of $\times 5,000$ (1) and $\times 20,000$ (2) for the specimens solution-treated at 700°C for 10 min (a) and aged at 400°C for 20 min (b), 100 min (c), 1,000 min (d) and 20,000 min (e)



structure. Figure 5 shows the FE-SEM micrograph for the specimen aged at 400°C for 20,000 min. The element distribution in the solute-depleted matrix (M) layer and precipitate (P) layer marked by an arrow was analyzed with EDS analysis, and the results were shown in Table 2. In the solute-depleted matrix (M) layer, Ag increased apparently and Au increased slightly compared to the alloy composition of Table 1. On the other hand, Cu and Zn decreased apparently and Pd decreased slightly. The opposite was detected in the precipitate (P) layer of the lamellar structure. The decrease in Ag and increase in Cu and Zn was apparent, but the decrease in Au and increase in Pd was slight. The minor ingredients, Pt and Ir were not detected using EDS analysis. By considering the small discrepancy between P1 and P2 data, together with the XRD analysis which showed that the final stable phases were two phases, Ag–Au-rich α_1 and AuCu I, it could be thought that P1 data inevitably included relatively large amounts of Ag of the surrounding solute-depleted matrix layer due to the large sampling spot size.

From the discussion above, it was clear that the solute-depleted matrix layer of the lamellar structure was composed of the Ag–Au-rich phase which was Cu-, Pd- and Zn-depleted compared to the parent α_0 phase. The precipitate layer of the lamellar structure was composed of the AuCu I ordered phase containing Pd and Zn. The distribution of Au was slightly unequal in the alternate Ag-rich and Cu-rich layers of the lamellar structure from the EDS analysis. By comparing the reported lattice parameter of the AuCu I phase ($a=0.3966$ nm, $c/a=0.926$) with the value obtained in the present study ($a_{200}=0.3940$ nm, $c/a=0.928$), such an unequal distribution of Au was thought to result from the fact that Au was partly replaced by Pd and Zn of which the atomic size is smaller than Au and larger than Cu in the AuCu I phase [20, 21].

Zn is one of the minor ingredients added in dental casting gold-based and silver-based alloys because it is a well-known deoxidizer. In a dental commercial low-gold alloy aged at

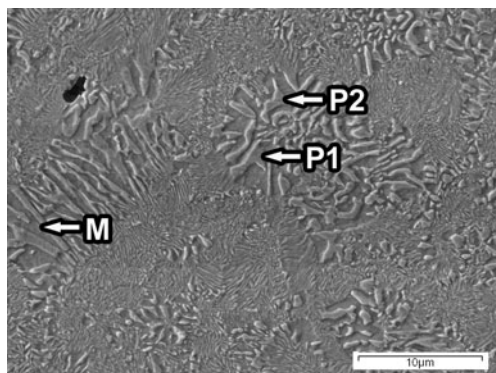


Fig. 5 FE-SEM micrograph for the specimen aged at 400°C for 20,000 min

Table 2 EDS analysis at the regions marked in Fig. 5 for the specimen aged at 400°C for 20,000 min

Region (at.%)	Au	Ag	Cu	Pd	Zn
M	40.5	46.6	8.0	4.8	0.1
P1	33.8	9.1	41.6	10.3	5.2
P2	33.6	2.8	46.1	8.6	8.9

400°C after solution treatment at 900°C and in a dental commercial Ag–Pd-based alloy aged at 350°C after solution treatment at 750°C, the minor ingredient, Zn—having relatively low melting temperature—tended to form extra phases preferably with Pd which is having relatively high melting temperature [2, 22]. However, in the equiatomic AuCu alloy, the single AuCu phase was made with Zn addition up to 20 at% at 300°C and 350°C after solution treatment at 500°C [23]. Moreover, the addition of Zn to the AuCu system promoted the AuCu-type ordering, and stabilized the AuCu-type structure, which made it possible for the AuCu–Zn alloy to have an excellent age-hardening [23–26]. In the present study, Zn was concentrated in the AuCu I layer containing Pd without formation of an extra phase. Such a Zn partitioning in the AuCu I phase was thought to have accelerated the AuCu-type ordering in the present study.

Summary

The age-hardening and overaging mechanisms related to the metastable phase formation by the decomposition of Ag and Cu in a dental casting gold alloy composed of 56Au–25Ag–11.8Cu–5Pd–1.7Zn–0.4Pt–0.1Ir (wt.%) were elucidated via hardness test, XRD study, FE-SEM observation and EDS analysis. The results are as follows:

1. The fast and apparent increase in hardness at the initial stage of the aging process at 400°C was caused by the nucleation and growth of the metastable Ag–Au-rich phase and the Cu–Au-rich phase by the miscibility limit of Ag and Cu.
2. The transformation of the metastable Ag–Au-rich α'_1 phase into the stable Ag–Au-rich α_1 phase progressed concurrently with the ordering of the Cu–Au-rich phase into the AuCu I phase through the metastable state, which resulted in the subsequent increase in hardness.
3. The further increase in hardness was restrained before complete decomposition of the parent α_0 phase due to the initiation of the lamellar-forming grain boundary reaction.
4. The lamellar-forming grain boundary reaction was not directly connected with the progress of the phase transformation of the metastable phases into the final product phases.

5. The heterogeneous expansion of the lamellar structure from the grain boundary caused greater softening than the subsequent further coarsening of the lamellar structure.

Open Access This article is distributed under the terms of the Creative Commons Attribution License which permits any use, distribution and reproduction in any medium, provided the original author(s) and source are credited.

References

1. Yasuda K (1987) Age-hardening and related phase transformations in dental gold alloys. *Gold Bull* 20:90–103
2. Noh DJ, Lee DH, Cho MH, Kim HI, Kwon YH, Seol HJ (2010) Phase transformation and microstructural changes during aging process in Ag–Pd–Cu–Pt–Zn alloy. *Mater Sci Technol* 26:203–209
3. Yu CH, Park MG, Kwon YH, Seol HJ, Kim HI (2007) Age-hardening behaviour and related phase transformation of a commercial type III dental casting gold alloy. *J Kor Res Soc Dent Mater* 34:217–226
4. Lee JH, Yi SJ, Seol HJ, Kwon YH, Lee JB, Kim HI (2006) Age-hardening by metastable phases in an experimental Au–Ag–Cu–Pd alloy. *J Alloys Compd* 425:210–215
5. Tani T, Udoh K, Yasuda K, Van Tendeloo G, Van Landuyt J (1991) Age-hardening mechanisms in a commercial dental gold alloy containing platinum and palladium. *J Dent Res* 70:1350–1357
6. Ohta M, Shiraishi T, Yamane M, Yasuda K (1983) Age-hardening mechanism of equiatomic AuCu and AuCu–Ag pseudo-binary alloys. *Dent Mater J* 2:10–17
7. Park MG, Yu CH, Seol HJ, Kwon YH, Kim HI (2008) Age-hardening behaviour of a spinodally decomposed low-carat gold alloy. *J Mater Sci* 43:1539–1545
8. Prince A, Raynor GV, Evans DS (1990) Phase diagrams of ternary gold alloys. *The Institute of Metals*, London, p 18
9. Massalski TB (1990) Binary alloy phase diagrams, 2nd edn. ASM International, Materials Park, pp 12–13, 28–29, 358–362
10. Seol HJ, Noh DJ, Lee SH, Kwon YH, Kim HI (2008) Age-hardening by the formation of metastable phases in an In-added Au–Ag–Cu–Pd alloy. *Mater Charact* 59:1190–1195
11. Jeon GH, Kwon YH, Seol HJ, Kim HI (2008) Hardening and overaging mechanisms in an Au–Ag–Cu–Pd alloy with In additions. *Gold Bull* 41:257–263
12. Kim HI, Jeon GH, Yi SJ, Kwon YH, Seol HJ (2007) Hardening and overaging mechanism of a commercial Au–Ag–Cu–Pd dental alloy. *J Alloys Compd* 441:124–130
13. Pan LG, Wang JN (2007) Age-hardening behavior of a low-gold dental alloy. *J Mater Sci* 18:171–177
14. Tanaka Y, Udoh K, Hisatsune K, Yasuda K (1998) Early stage of ordering in stoichiometric AuCu alloy. *Mater Trans JIM* 39:87–94
15. Kawashima I, Ohno H, Sarkar NK (2000) Effect of Pd or Au addition on age-hardening in AgMn-based alloys. *Dent Mater* 16:75–79
16. Suryanarayana C, Norton MG (2003). *X-ray diffraction: A practical approach*, 1st edn. Springer Science & Business Media, New York, pp 207–210
17. Hisatsune K, Udoh KI (1991) Age-hardening characteristics in an AuCu–14at% Ag alloy. *J Alloys Compd* 176:269–283
18. Kim HI, Jang MI, Kim MS (1999) Age-hardening associated with grain boundary precipitation in a commercial dental gold alloy. *J Oral Rehabil* 26:215–222
19. Lee HK, Moon HM, Seol HJ, Lee JE, Kim HI (2004) Age hardening by dendrite growth in a low-gold dental casting alloy. *Biomaterials* 25:3869–3875
20. Villars P, Calvert LD (1985) Pearson's handbook of crystallographic data for intermetallic phases. American Society for Metals, Metals Park, p 1198
21. Cullity BD (1978) Elements of X-ray diffraction, 2nd edn. Addison-Wesley Publishing, Massachusetts, pp 506–507
22. Seol HJ, Kim GC, Son KH, Kwon YH, Kim HI (2005) Hardening mechanism of an Ag–Pd–Cu–Au dental casting alloy. *J Alloys Compd* 387:139–146
23. Seol HJ, Shiraishi T, Tanaka Y, Miura E, Hisatsune K, Kim HI (2002) Ordering behaviors and age-hardening in experimental AuCu–Zn pseudobinary alloys for dental applications. *Biomaterials* 23:4873–4879
24. Labarge JJ (1979) Hardening of gold-based dental casting alloys. *Gold Bull* 12:46–52
25. Sato H, Toth RS (1961) Effect of additional elements on the period of CuAu II and the origin of the long-period superlattice. *Phys Rev* 124:1833–1847
26. Ogawa S, Watanabe D, Watanabe H, Komoda T (1959) Anti-phase domains in gold–copper–zinc ordered alloys revealed by electron microscope. *J Phys Soc Jpn* 14:936–941